



STABILITY OF SEMI-RIGID PORTAL FRAMES WITH TAPERED COLUMNS AND LATERAL SUPPORT

M. Rezaiee-Pajand*, F. Shahabian and M. Bambaeechee
Department of Civil Engineering, Ferdowsi University of Mashhad, Iran

Received: 5 March 2014; **Accepted:** 10 October 2014

ABSTRACT

An exact formulation for computing the critical buckling load of semi-rigid steel frames with tapered columns will be obtained. The presented methodology is based on the precise solution of the governing differential equations for elastic buckling of the uniform and non-uniform frames. These formulations also can be used for the tapered column with various support conditions. Moreover, the effect of tapered columns, with parabolic and quadratic functions for variation of the moment of inertia, flexibility of connections, and lateral support, such as bracing, on the equivalent buckling length factor of the frame will be studied parametrically as well as numerically. Comparing the findings with the available results indicates the accuracy, validity and capabilities of the proposed approach.

Keywords: Stability analysis; tapered columns; semi-rigid connections; steel frames; equivalent buckling length factor; critical buckling load.

1. INTRODUCTION

Tapered or non-prismatic members have been extensively used in structural, mechanical and aeronautical engineering. The elastic, inelastic, fracture, and damage theories on the stability of structures were presented by Bažant and Cedolin [1]. Another famous book on the theory of elastic stability was written by Timoshenko and Gere [2]. The stability design of steel frames was investigated by Chen and Lui [3]. For the first time, Euler calculated accurately the column buckling load [4]. Stability analysis of tapered columns and 2D frames incorporating non-uniform members has been studied during the last century, and it still remains an important research topic. Closed-form buckling solutions for several special types of non-prismatic columns with simple boundary conditions are given by Gere and Carter [5]. In the field of analytical solutions, many investigations are based on the assumed stiffness distributions. Ermopoulos and Kounadis dealt with simple portal braced and un-braced frames comprising tapered lattice columns by using a second-order polynomial

* E-mail address of the corresponding author: rezaiee@um.ac.ir (M. Rezaiee Pajand)

stiffness variation [6]. They found a closed-form buckling load via bifurcation analysis. Moreover, Raftoyiannis and Ermopoulos studied the effect of initial imperfections on the stability of tapered members [7]. In another event, Ermopoulos studied buckling length of framed compression members with semi-rigid connections [8].

A general power series approach can be found in Refs. [9,10], where the expressions for stability functions of a general non-prismatic member are given. Another solution for a general stiffness distribution column, using Bessel functions, has been presented by Li [11,12]. In these works, the expression for describing the distribution of flexural stiffness is arbitrary. Coşkun and Atay used a variational iteration method (VIM) to obtain the buckling load of non-uniform columns under the constant axial loading [13]. They used exponential function and power law for variation of flexural rigidity. Based on the Wentzel-Kramers-Brillouin (WKB) method, Darbandi et al. presented the closed-form solution for the buckling of variable section column under axial loading, recently [14].

The other researchers have worked with the approximate techniques. O'Rourke and Zebrowski studied the buckling load of a non-uniform member by the finite difference method [15]. Similarly, Iremonger used a finite difference strategy to determine the buckling loads for tapered and stepped column [16]. For quick calculation of the critical load of tapered members and plane steel frames with tapered members, an approximate method was presented by Bazeos and Karabalis [17]. Li and Li used a generalized finite element in the buckling analysis of tapered lattice column [18]. More recently, Marques et al. developed a consistent buckling design procedure for taper columns based on the finite element method [19].

As it was mentioned by the researchers, the interest in obtaining more accurate and efficient results, using analytical or semi-analytical tools remains strong, even in the presence of some simplifying assumptions pertaining to geometry, loading or boundary conditions [20-24]. Based on this brief review, it can be seen that the comprehensive studies on the stability of non-prismatic column have been performed rather than non-uniform frames. Moreover, no attempt has been made for considering the joint flexibility and elastic bracing system in steel portal frames with tapered members, so far. The purpose of this study is to derive the exact expression, accounting for aforementioned parameters, for computing the critical buckling load of the frame. The outcomes presented here in can be readily used for stability design of the portal frame with tapered members. In fact, the critical buckling load and corresponding equivalent buckling length factor of semi-rigid portal frames will be calculated. Furthermore, the effect of tapered columns, flexibility of connections, and lateral support such as bracings on the stability of the frame will be investigated.

2. STABILITY ANALYSIS

It is intended to analysis the portal frames shown in Fig. 1. The frame in Fig. 1(a) has two pinned supports; while the frame in Fig. 1(b) is based on two fixed supports. Columns have both length l_c , and moment of inertia is assumed to vary in the following form:

$$I_i(x_i) = I_c \left(\frac{x_i}{a} \right)^n \quad (i = 1,3) \tag{1}$$

In this function $I_i(x_i)$ is the moment of inertia of the cross-section at a distance x_i from the origin, as shown in Fig. 1, and I_c is the moment of inertia at a distance a from the origin. According to Table (1), the shape factor, n , is equal to 2 for tapered members with varying depth and constant cross-sectional area, such as tower and open-web sections, whereas for solid circular and square sections, with varying diameter and dimension along their axis, respectively, this factor equals to 4. It should be noted, for the uniform member, the shape factor n is equal to zero. The beam has length l_b , and moment of inertia I_b . Each frame is subjected to two vertical concentrated loads, P_1 and P_3 , on the centerline of columns. The beam is connected to columns via semi-rigid connections. It is assumed that both beam-to-column connections, has rotational stiffness K_c . The lateral elastic support is modeled by a horizontal spring with axial stiffness K_b , which is located at the top of the right column.

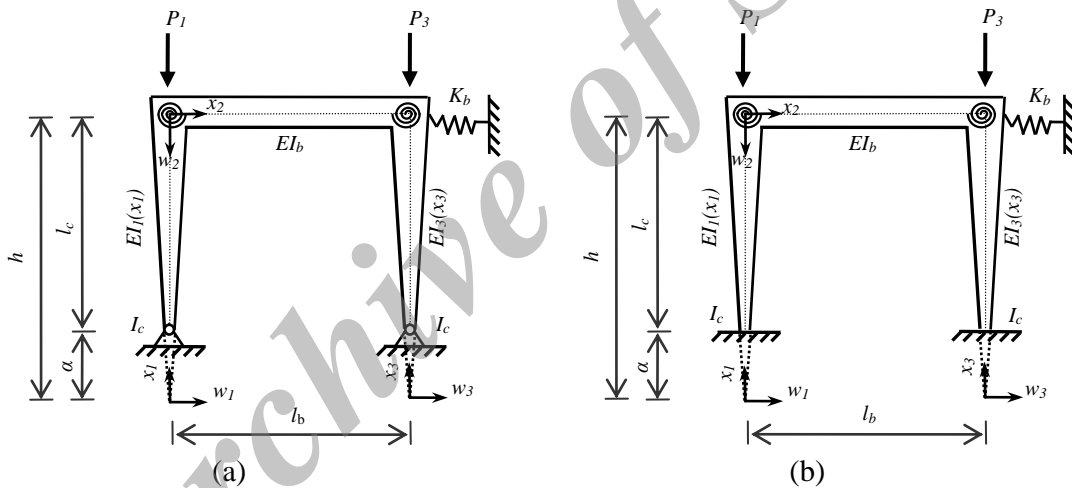
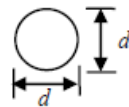
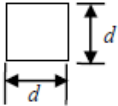
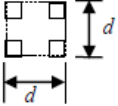
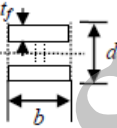


Figure 1. Geometry and sign convention of non-uniform frames with: (a) pinned supports, and (b) fixed supports

Table 1: Various cross sections and their associated shape factors for linear tapers [5]

Shape	Shape factor (n)
Solid circular section (Varying diameter, d)	4



Solid square section (Varying dimension, d)		4
Tower section (Constant areas concentrated near corners Varying dimension, d)		2
Open –web section (Constant dimensions b, t_f Varying depth, d)		2

Within the limitations of the beam-column theory, the governing fourth-order differential equations for the columns and the beam are given below:

$$\left. \begin{aligned} \frac{d^2}{dx_1^2} \left[EI_c \left(\frac{x_1}{a} \right)^n \frac{d^2 w_1}{dx_1^2} \right] + P_1 \frac{d^2 w_1}{dx_1^2} &= 0 \\ \frac{d^2}{dx_2^2} \left[EI_b \frac{d^2 w_2}{dx_2^2} \right] &= 0 \\ \frac{d^2}{dx_3^2} \left[EI_c \left(\frac{x_3}{a} \right)^n \frac{d^2 w_3}{dx_3^2} \right] + P_3 \frac{d^2 w_3}{dx_3^2} &= 0 \end{aligned} \right\} \quad (2)$$

The general solutions of Eq. (2) for $n = 0, 2$ and 4 are presented in Eqs. (3) up to (5), respectively.

$$\left. \begin{aligned} w_1 &= A_1 \sin \rho x + B_1 \cos \rho x + C_1 x + D_1 \\ w_2 &= A_2 x^3 + B_2 x^2 + C_2 x + D_2 \\ w_3 &= A_3 \sin \rho x + B_3 \cos \rho x + C_3 x + D_3 \end{aligned} \right\} , \quad \left(\rho = \sqrt{\frac{Pl_c^2}{EI_c}} \right) \quad (3)$$

$$\left. \begin{aligned} w_1 &= \sqrt{\frac{x}{a}} \left\{ A_1 \sin \left[\rho Ln \left(\frac{x}{a} \right) \right] + B_1 \cos \left[\rho Ln \left(\frac{x}{a} \right) \right] \right\} + C_1 x + D_1 \\ w_2 &= A_2 x^3 + B_2 x^2 + C_2 x + D_2 \\ w_3 &= \sqrt{\frac{x}{a}} \left\{ A_3 \sin \left[\rho Ln \left(\frac{x}{a} \right) \right] + B_3 \cos \left[\rho Ln \left(\frac{x}{a} \right) \right] \right\} + C_3 x + D_3 \end{aligned} \right\} , \quad \left(\rho = \sqrt{\frac{Pa^2}{EI_c} - \frac{1}{4}} \right) \quad (4)$$

$$\left. \begin{aligned} w_1 &= A_1 x \sin\left(\frac{\rho a}{x}\right) + B_1 x \cos\left(\frac{\rho a}{x}\right) + C_1 x + D_1 \\ w_2 &= A_2 x^3 + B_2 x^2 + C_2 x + D_2 \\ w_3 &= A_3 x \sin\left(\frac{\rho a}{x}\right) + B_3 x \cos\left(\frac{\rho a}{x}\right) + C_3 x + D_3 \end{aligned} \right\}, \quad \left(\rho = \sqrt{\frac{Pa^2}{EI_c}} \right) \quad (5)$$

where A_i , B_i , C_i , and D_i ($i=1,2,3$) are integration constants to be determined using boundary and kinematic conditions. These constants can be calculated based on Tables (2) and (3) for prismatic and non-prismatic columns, respectively.

Table 2: Kinematic and boundary conditions of a simple frame with prismatic columns

Pinned- supports		Fixed- supports	
Boundary conditions	Kinematic conditions	Boundary conditions	Kinematic conditions
$w_1(0) = 0$	$w_1(h) = w_3(h)$	$w_1(0) = 0$	$w_1(h) = w_3(h)$
$w_1''(0) = 0$	$V_1(h) + V_3(h) + K_b w_3(h) = 0$	$w_1'(0) = 0$	$V_1(h) + V_3(h) + K_b w_3(h) = 0$
$w_2(0) = 0$	$M_1(h) - M_2(0) = 0$	$w_2(0) = 0$	$M_1(h) - M_2(0) = 0$
$w_2(l_b) = 0$	$M_2(0) = K_c [w_1'(h) - w_2'(0)]$	$w_2(l_b) = 0$	$M_2(0) = K_c [w_1'(h) - w_2'(0)]$
$w_3(0) = 0$	$M_2(l_b) + M_3(h) = 0$	$w_3(0) = 0$	$M_2(l_b) + M_3(h) = 0$
$w_3''(0) = 0$	$M_2(l_b) = K_c [w_2'(l_b) - w_3'(h)]$	$w_3'(0) = 0$	$M_2(l_b) = K_c [w_2'(l_b) - w_3'(h)]$

Table 3: Kinematic and boundary conditions of a simple frame with non-prismatic columns

Pinned- supports		Fixed- supports	
Boundary conditions	Kinematic conditions	Boundary conditions	Kinematic conditions
$w_1(a) = 0$	$w_1(h) = w_3(h)$	$w_1(a) = 0$	$w_1(h) = w_3(h)$
$w_1''(a) = 0$	$V_1(h) + V_3(h) + K_b w_3(h) = 0$	$w_1'(a) = 0$	$V_1(h) + V_3(h) + K_b w_3(h) = 0$

$w_2(0) = 0$	$M_1(h) - M_2(0) = 0$	$w_2(0) = 0$	$M_1(h) - M_2(0) = 0$
$w_2(l_b) = 0$	$M_2(0) = K_c[w'_1(h) - w'_2(0)]$	$w_2(l_b) = 0$	$M_2(0) = K_c[w'_1(h) - w'_2(0)]$
$w_3(a) = 0$	$M_2(l_b) + M_3(h) = 0$	$w_3(a) = 0$	$M_2(l_b) + M_3(h) = 0$
$w_3''(a) = 0$	$M_2(l_b) = K_c[w'_2(l_b) - w'_3(h)]$	$w_3'(a) = 0$	$M_2(l_b) = K_c[w'_2(l_b) - w'_3(h)]$

In practice, both columns in a simple frame have the same sectional properties (i.e. $I(x_1)=I(x_3)$), and mostly loaded by equal compression forces (i.e. $P_1 \approx P_3$). Accordingly, it is assumed that $P_1=P_3=P$ and $I_1=I_3$. At this stage, by employing the boundary and kinematic conditions, and also the coming non-dimensional parameters, $\rho^2 = \frac{Pa^2}{EI_c}$, $\nu = \frac{I_c l_b}{I_b h}$, $r = \frac{a}{h}$, $K_b^* = \frac{K_b h^3}{EI_c} r^2$, $K_c^* = \frac{K_c l_b}{EI_b}$, the following system of dimensionless equations can be found, when the shape factor, n , is equal to 4:

$$\left. \begin{aligned}
 & r(A_1 \sin \rho + B_1 \cos \rho + C_1) + \bar{D}_1 = 0 \\
 & \rho^2 (A_1 \sin \rho + B_1 \cos \rho) = 0 \\
 & r(A_3 \sin \rho + B_3 \cos \rho + C_3) + \bar{D}_3 = 0 \\
 & -\rho^2 (A_3 \sin \rho + B_3 \cos \rho) = 0 \\
 & \nu(A_2 \nu + B_2 + C_2) = 0 \\
 & \sin(r\rho)(A_1 - A_3) + \cos(r\rho)(B_1 - B_3) + (C_1 - C_3) + (\bar{D}_1 - \bar{D}_3) = 0 \\
 & -\rho^2 (C_1 + C_3) + K_b^* (A_3 \sin(r\rho) + B_3 \cos(r\rho) + C_3 + \bar{D}_3) = 0 \\
 & \rho^2 (A_1 \sin(r\rho) + B_1 \cos(r\rho)) + 2B_2 r^2 = 0 \\
 & K_c^* [\sin(r\rho)(B_1 \rho - A_1) + \cos(r\rho)(A_1 \rho + B_1) + (C_1 - C_2)] + 2B_2 \nu = 0 \\
 & -2r^2 (3A_2 \nu + B_2) + \rho^2 (A_3 \sin(r\rho) + B_3 \cos(r\rho)) = 0 \\
 & 2\nu(3A_2 \nu + B_2) + K_c^* [\nu(3A_2 \nu + 2B_2) + (A_3 \rho - B_3) \cos(r\rho) - (A_3 + B_3 \rho) \sin(r\rho) + (C_2 - C_3)] = 0
 \end{aligned} \right\} \quad (6)$$

$$\left. \begin{aligned}
 &r(A_1 \sin \rho + B_1 \cos \rho + C_1) + \bar{D}_1 = 0 \\
 &\sin \rho(A_1 + B_1 \rho) + \cos \rho(B_1 - A_1 \rho) + C_1 = 0 \\
 &r(A_3 \sin \rho + B_3 \cos \rho + C_3) + \bar{D}_3 = 0 \\
 &\sin \rho(A_3 + B_3 \rho) + \cos \rho(B_3 - A_3 \rho) + C_3 = 0 \\
 &\nu(A_2 \nu + B_2 + C_2) = 0 \\
 &\sin(r\rho)(A_1 - A_3) + \cos(r\rho)(B_1 - B_3) + (C_1 - C_3) + (\bar{D}_1 - \bar{D}_3) = 0 \\
 &-\rho^2(C_1 + C_3) + K_b^*(A_3 \sin(r\rho) + B_3 \cos(r\rho) + C_3 + \bar{D}_3) = 0 \\
 &\rho^2(A_1 \sin(r\rho) + B_1 \cos(r\rho)) + 2B_2 r^2 = 0 \\
 &K_c^*[\sin(r\rho)(B_1 \rho - A_1) + \cos(r\rho)(A_1 \rho + B_1) + (C_1 - C_2)] + 2B_2 \nu = 0 \\
 &-2r^2(3A_2 \nu + B_2) + \rho^2(A_3 \sin(r\rho) + B_3 \cos(r\rho)) = 0 \\
 &2\nu(3A_2 \nu + B_2) + K_c^*[\nu(3A_2 \nu + 2B_2) + (A_3 \rho - B_3) \cos(r\rho) - (A_3 + B_3 \rho) \sin(r\rho) + (C_2 - C_3)] = 0
 \end{aligned} \right\} \quad (7)$$

with respect to the dimensionless constants $A_1, B_1, C_1, \bar{D}_1 = D_1/h, A_2, B_2, C_2, A_3, B_3, C_3, \bar{D}_3 = D_3/h$. It should be noted that Eqs. (6) and (7) belong to pinned and fixed supports, respectively. By setting the determination of last equations to zero, and subsequently, the critical buckling load of the non-uniform semi-rigid frames with shape factor $n=4$, will be obtained:

$$\det[K_i] = 0 \quad (i = 1,2) \quad (8)$$

The matrices $[K_i]$ ($i=1,2$) are given explicitly in Appendix A (see Eqs. (A1) and (A2)). Similarly, the stability matrices when the shape factor, n , is equal to 2 will be derived. Subsequently, the critical buckling load of the mentioned frame with pinned and fixed bases can be found by setting the determination of the stability matrices equal to zero:

$$\det[K_i] = 0 \quad (i = 3,4) \quad (9)$$

The matrices \mathbf{K}_3 and \mathbf{K}_4 are presented explicitly in Appendix A (see Eqs. (A3) and (A4)). Furthermore, the corresponding matrices, $[K_i]$ ($i=5,6$), for the uniform frames with pinned and fixed supports, are given explicitly in Appendix A (see Eqs. (A5) and (A6)). Accordingly, the critical buckling load of the these frame, could be respectively obtained as follows:

$$\det[K_i] = 0 \quad (i = 5,6) \quad (10)$$

By solving Eqs. (8) up to (10), the non-dimensional critical buckling load, ρ_{cr} , is obtained, and consequently, the following critical buckling load of the frame is computed:

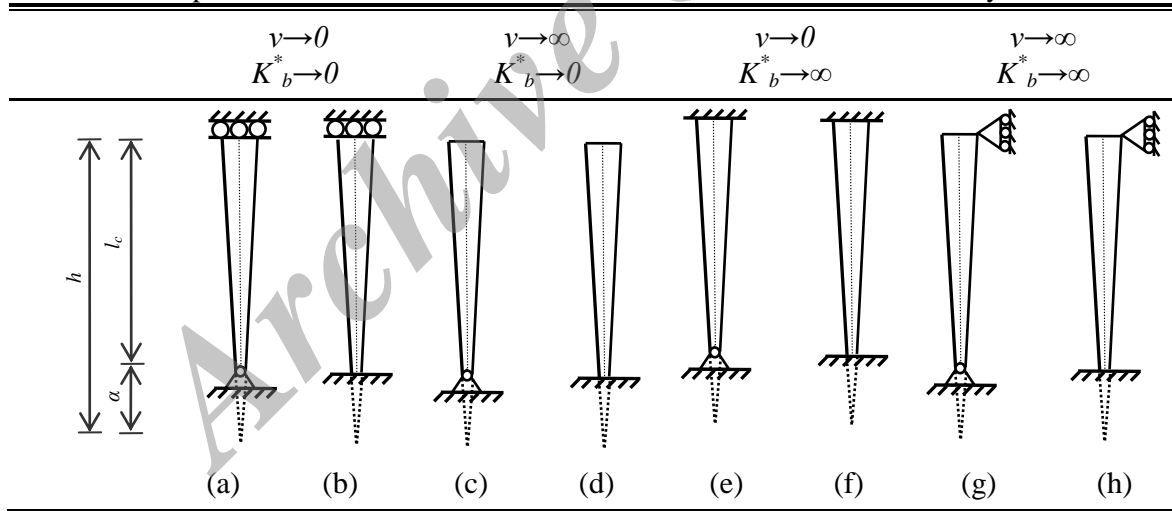
$$P_{cr} = \frac{\pi^2 EI_m}{(Kl_c)^2} = \begin{cases} \rho_{cr}^2 \frac{EI_c}{a^2} & \text{for } n=4 \\ \left(\rho_{cr}^2 + \frac{1}{4}\right) \frac{EI_c}{a^2} & \text{for } n=2 \\ \rho_{cr}^2 \frac{EI_c}{l_c^2} & \text{for } n=0 \end{cases} \quad (11)$$

Moreover, Eq. (11) leads to the equivalent buckling length factor, k , of the column, which has the next value:

$$k = \frac{\pi}{\sqrt{P_{cr}^*}} \quad (12)$$

It should be mentioned that $P_{cr}^* = P_{cr} l_c^2 / EI_m$, and I_m is the moment of inertia at the middle of the column (i.e. for $x = a + 0.5l_c$). It is reminded that, if one assume the limit values of v and K_b^* , this method can be used for the single non-uniform column. These particular cases are given in Table (4).

Table 4: Tapered column with limit value of v and K_b^* and variant end boundary conditions



3. THE BEHAVIOR OF CONNECTIONS

Commonly, the moment-rotation relationship describes the behavior of connections [3]. In the present investigation, it is assumed that the semi-rigid connections have a linear behavior. The basic equation for the linear model is defined as follows:

$$M = K_c \theta \quad (13)$$

In this equation, M is the moment and K_c and θ are the rotational stiffness and rotation of the connection, respectively. The rotational stiffness of the connection, K_c , could be considered as either the initial stiffness or the secant connection stiffness.

4. PARAMETRIC STUDY

Solving numerically the buckling equations Eqs. (8) through (10), the dimensionless critical buckling load factor, ρ_{cr} , can be computed for the frame with non-uniform ($n=4$ and 2) and uniform ($n=0$) columns, respectively. This solution is valid for any desired combination of the defined non-dimensional parameters, namely the stiffness ratio ν , the dimensionless rotational stiffness of semi-rigid connections K_c^* , and the dimensionless axial stiffness of lateral elastic support K_b^* . The stiffness ratio ν varies up to 4 , which is a reasonable range of beam-column characteristic properties for commonly designed steel frames. Concerning the rotational stiffness values of the connections (K_c^*), numerical results are presented for relatively low quantities ($K_c^* = 0.1, 0.5, 1.0$), that correspond to bolted connections with low rigidity, as well as for higher ones ($K_c^* = 5, 10, \infty$), that correspond to more rigid connections such as welded joints. Regarding the axial stiffness values of the lateral elastic support K_b^* , numerical responses are obtained for minimum value ($K_b^* = 0$) and relatively intermediate amounts ($K_b^* = 1, 10$), that correspond to un-braced and semi-braced frames, respectively, as well as for maximum ones ($K_b^* = \infty$) that correspond to fully-braced frames. It should be added, for tapered column, the taper ratio, r , varies in the range of $0 < r \leq 1$, where $r = 1$ denote a uniform member and if $r \rightarrow 0$, the member would taper to a point at the base, which is only a theoretical limit and is not practical.

4.1 Uniform section ($n=0$)

The variation of the equivalent buckling length factor k , for the uniform frame with pinned supports, with respect to stiffness ratio ν for various values of the rotational stiffness K_c^* , and various amounts of the lateral support stiffness K_b^* , are plotted in Fig. 2.

According to Fig. 2(a), in the case of the un-braced frame (i.e. $K_b^* = 0$), with pinned supports and $\nu \rightarrow 0$, the equivalent buckling length factor tends to $k \rightarrow 2$, irrespective of the rotational stiffness K_c^* values. This case corresponds to a pinned-fixed sway column (see case (a) in Table (4)). Also, as the stiffness ratio $\nu \rightarrow \infty$, the equivalent buckling length factor tends to $k \rightarrow \infty$ for all cases of K_c^* .

For intermediate values of the stiffness ratio ν and low rotational stiffness amounts (i.e. $K_c^* = 0.1, 0.5$ and 1) there is a substantial increase of the equivalent buckling length factor k , which is more pronounced when ν tends to low values. This effect is reversed in the case of high rotational stiffness quantities (i.e. $K_c^* = 5, 10$ and ∞) as ν tends to high values. The same pattern pronounces also in the cases when a lateral support is present (i.e. $K_b^* \neq 0$), as shown in Figs. 2(b) up to 2(d).

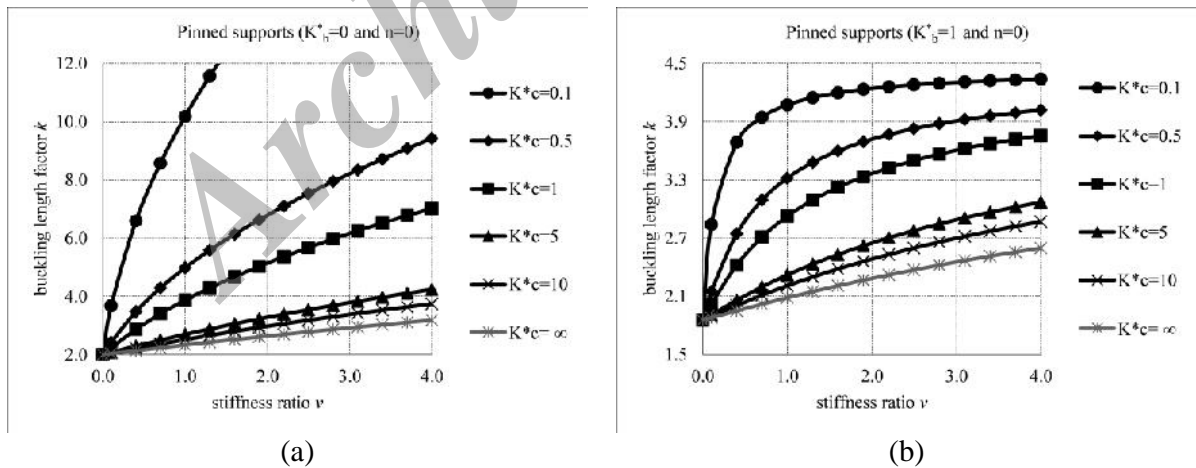
In addition, regardless of the rotational stiffness K_c^* quantities, when the stiffness ratio

tends to $\nu \rightarrow 0$, the equivalent buckling length factor tends to $k \rightarrow 1.854, 1.243$ and 0.699 for $K_b^* \rightarrow 1, 10$ and ∞ , respectively. The latter case corresponds to a pinned-fixed non-sway column (see case (e) in Table (4)). Also, for all cases of K_c^* when the stiffness ratio tends to $\nu \rightarrow \infty$, the equivalent buckling length factor tends to $k \rightarrow 4.339, 1.402$ and 1.000 for $K_b^* \rightarrow 1, 10$ and ∞ , respectively. This last case (i.e. $K_b^* \rightarrow \infty$) corresponds to a pinned-pinned non-sway column (see case (g) in Table (4)).

In Fig. 3, the same plots as above are depicted for the frame with fixed supports. More specifically, in the case of the un-braced frame (i.e. $K_b^* = 0$) with fixed supports and $\nu \rightarrow 0$, the equivalent buckling length factor tends to $k \rightarrow 1$, irrespective of the rotational stiffness K_c^* values. This case corresponds to a fixed-fixed sway column (see case (b) in Table (4)). On the other hand, for $\nu \rightarrow \infty$, the equivalent buckling length factor tends to $k \rightarrow 2$, also regardless of the K_c^* amounts. This case corresponds to a fixed-free sway column (see case (d) in Table (4)).

For intermediate values of the stiffness ratio ν and low rotational stiffness amounts (i.e. $K_c^* = 0.1, 0.5$ and 1) there is a significant increase of the equivalent buckling length factor k which is also more pronounced as ν tends to low values. The similar pattern appears also in the cases when an elastic bracing support is present (i.e. $K_b^* \neq 0$), as shown in Figs. 3(b) through 3(d).

It should be noted that regardless of the rotational stiffness K_c^* values, whenever the stiffness ratio tends to $\nu \rightarrow 0$, the buckling length factor tends to $k \rightarrow 0.980, 0.843$ and 0.500 for $K_b^* \rightarrow 1, 10$ and ∞ , respectively. The last case (i.e. $K_b^* \rightarrow \infty$) corresponds to a fixed-fixed non-sway column (see case (f) in Table (4)). On the other hand, for $\nu \rightarrow \infty$, the equivalent buckling length factor tends to $k \rightarrow 1.838, 1.237$ and 0.700 for $K_b^* \rightarrow 1, 10$ and ∞ , respectively. The latter case (i.e. $K_b^* \rightarrow \infty$) corresponding to a fixed-pinned non-sway column (see case (h) in Table (4)).



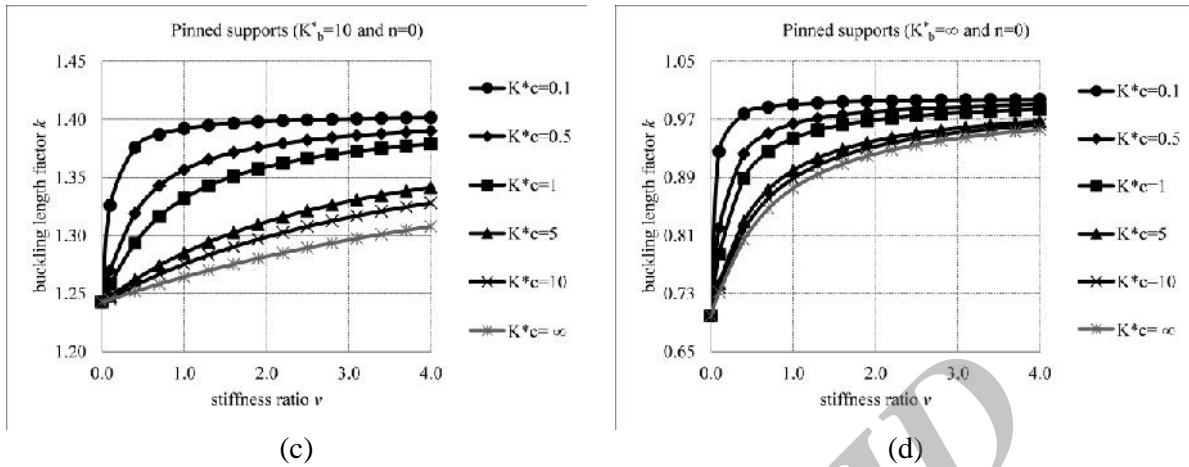


Figure 2: Buckling length factor k versus stiffness ratio v for pinned support frame with prismatic columns ($n=0$) and various values of K_c^* and K_b^*

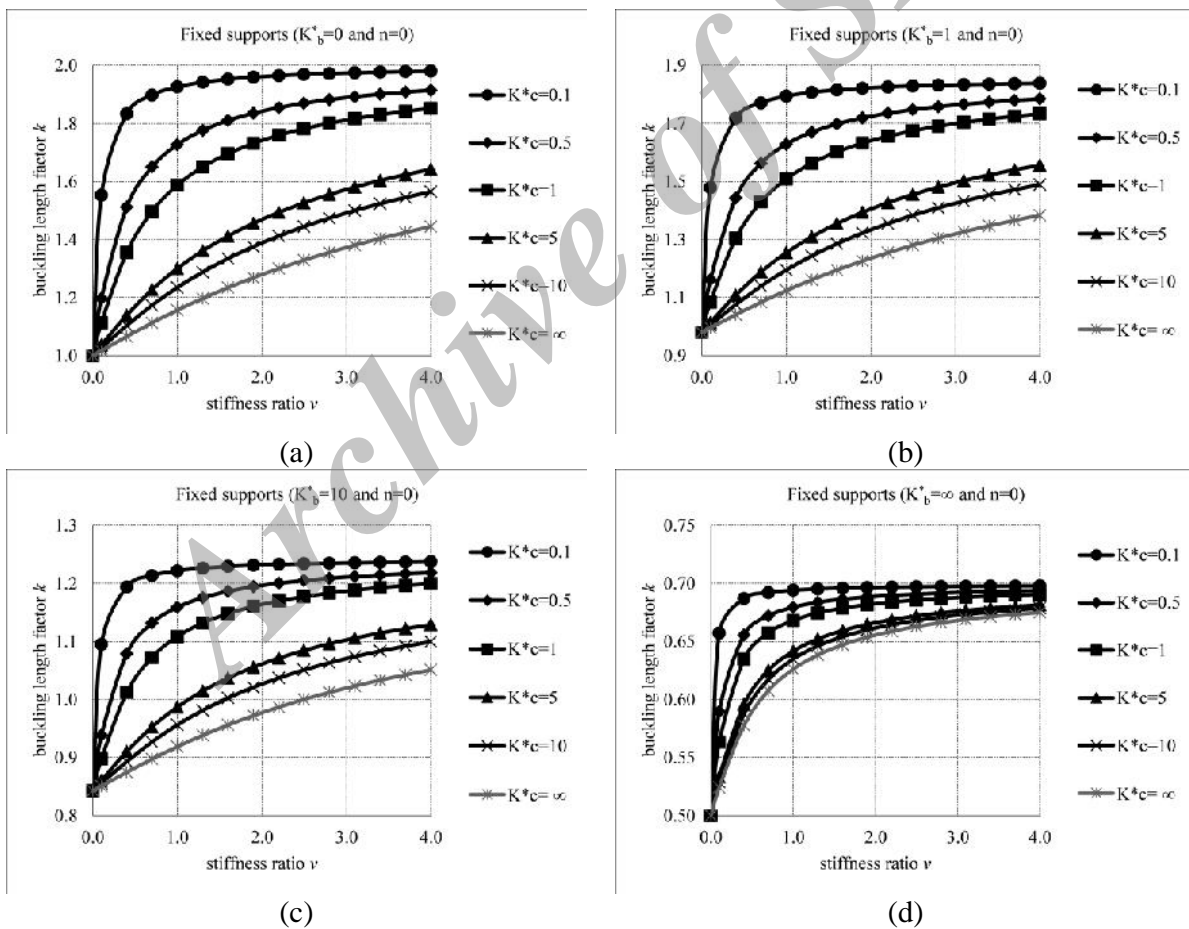


Figure 3: Buckling length factor k versus stiffness ratio v for fixed support frame with prismatic columns ($n=0$) and various values of K_c^* and K_b^*

4.2 Tower and open-web section ($n=2$)

In Fig. 4, the variation of the equivalent buckling length factor k , with respect to stiffness ratio ν for various quantities of the rotational stiffness K_c^* , and various values of the lateral support stiffness K_b^* , and $r=1/2$, are investigated for the non-uniform frame with pinned supports.

From Fig. 4(a), more specifically, in the case of the un-braced frame (i.e. $K_b^* = 0$), with pinned supports and $\nu \rightarrow 0$, the equivalent buckling length factor tends to $k \rightarrow 1.816$, regardless of the rotational stiffness K_c^* values. This case corresponds to a pinned-fixed sway column (see case (a) in Table (4)). Also, as the stiffness ratio $\nu \rightarrow \infty$, the equivalent buckling length factor tends to $k \rightarrow \infty$ for all cases of K_c^* . However, for the low values of the rotational stiffness in the un-braced frame, the solutions are unacceptable [6].

For intermediate amounts of the stiffness ratio ν and low rotational stiffness values (i.e. $K_c^*=0.1, 0.5$ and 1) there is a considerable increase of the equivalent buckling length factor k , which is more pronounced when ν tends to low quantities. This effect is reversed in the case of high rotational stiffness values (i.e. $K_c^*=5, 10$ and ∞) as ν tends to high values. The same pattern pronounces also in the cases when a lateral support is present (i.e. $K_b^* \neq 0$), as shown in Figs. 4(b) up to 4(d).

Moreover, regardless of the rotational stiffness K_c^* quantities, when the stiffness ratio tends to $\nu \rightarrow 0$, the equivalent buckling length factor tends to $k \rightarrow 1.810, 1.757$ and 0.726 for $K_b^* \rightarrow 1, 10$ and ∞ , respectively. This latter case corresponds to a pinned-fixed non-sway column (see case (e) in Table (4)). Also, for all cases of K_c^* when the stiffness ratio tends to $\nu \rightarrow \infty$, the equivalent buckling length factor tends to $k \rightarrow \infty, 5.904$ and 1.033 for $K_b^* \rightarrow 1, 10$ and ∞ , respectively. This last case (i.e. $K_b^* \rightarrow \infty$) corresponds to a pinned-pinned non-sway column (see case (g) in Table (4)).

In Fig. 5, the same plots as above are presented for the frame with fixed supports. In the case of the un-braced frame (i.e. $K_b^*=0$) with fixed supports and $\nu \rightarrow 0$, the equivalent buckling length factor tends to $k \rightarrow 1.033$, irrespective of the rotational stiffness K_c^* values. This case corresponds to a fixed-fixed sway column (see case (b) in Table (4)). On the other hand, for $\nu \rightarrow \infty$, the equivalent buckling length factor tends to $k \rightarrow 2.4$, also regardless of the K_c^* amounts. This case corresponds to a fixed-free sway column (see case (d) in Table (4)).

For intermediate values of the stiffness ratio ν and low rotational stiffness amounts (i.e. $K_c^*=0.1, 0.5$ and 1) there is a substantial increase of the equivalent buckling length factor k which is also more pronounced as ν tends to low values. The similar pattern appears also in the cases when an elastic bracing support is present (i.e. $K_b^* \neq 0$), as shown in Figs. 5(b) through 5(d).

It should be noted that regardless of the rotational stiffness K_c^* values, whenever the stiffness ratio tends to $\nu \rightarrow 0$, the buckling length factor tends to $k \rightarrow 1.032, 1.021$ and 0.521 for $K_b^* \rightarrow 1, 10$ and ∞ , respectively. The last case (i.e. $K_b^* \rightarrow \infty$) corresponds to a fixed-fixed non-sway column (see case (f) in Table (4)). On the other hand, for $\nu \rightarrow \infty$, the equivalent buckling length factor tends to $k \rightarrow 2.383, 2.247$ and 0.726 for $K_b^* \rightarrow 1, 10$ and ∞ , respectively. The latter case (i.e. $K_b^* \rightarrow \infty$) corresponding to a fixed-pinned non-sway column (see case (h) in Table (4)).

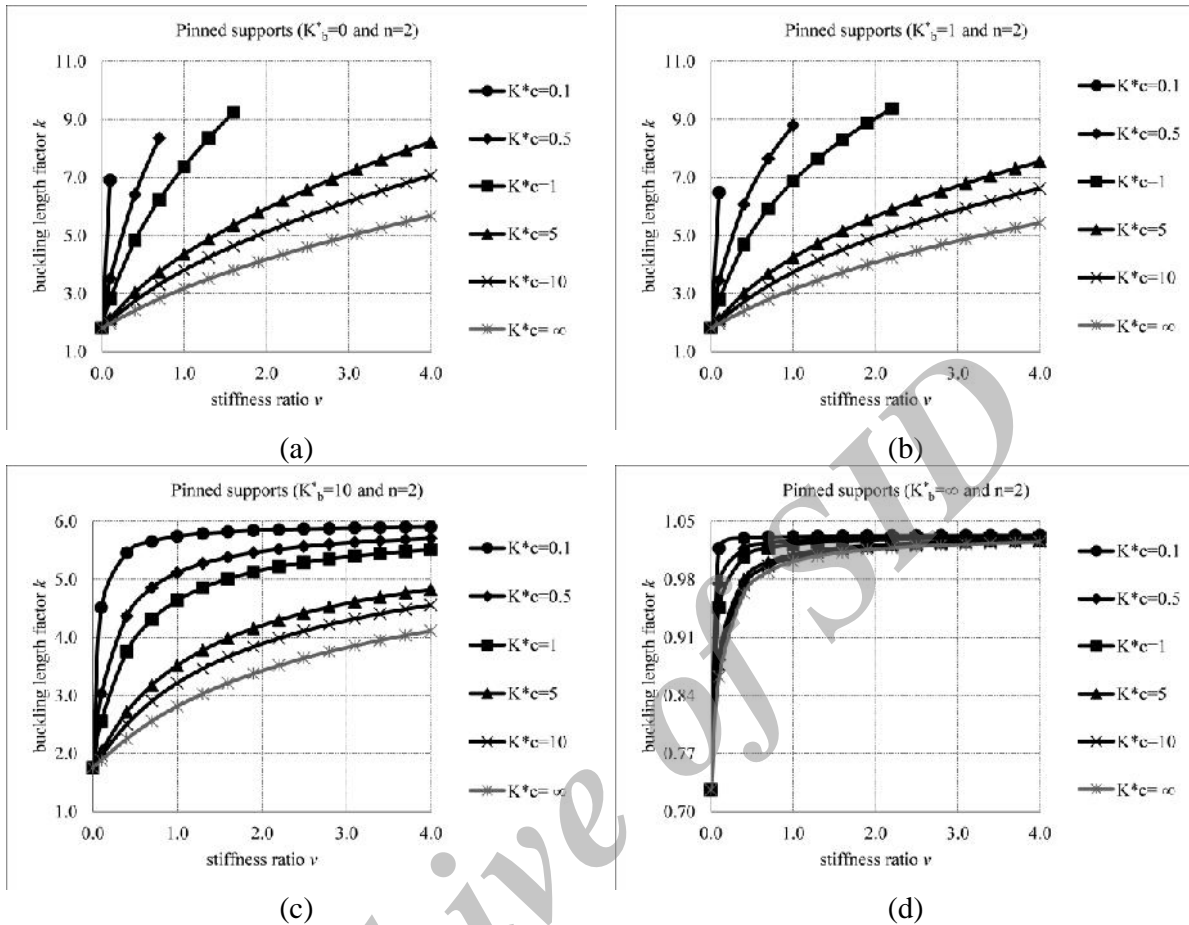
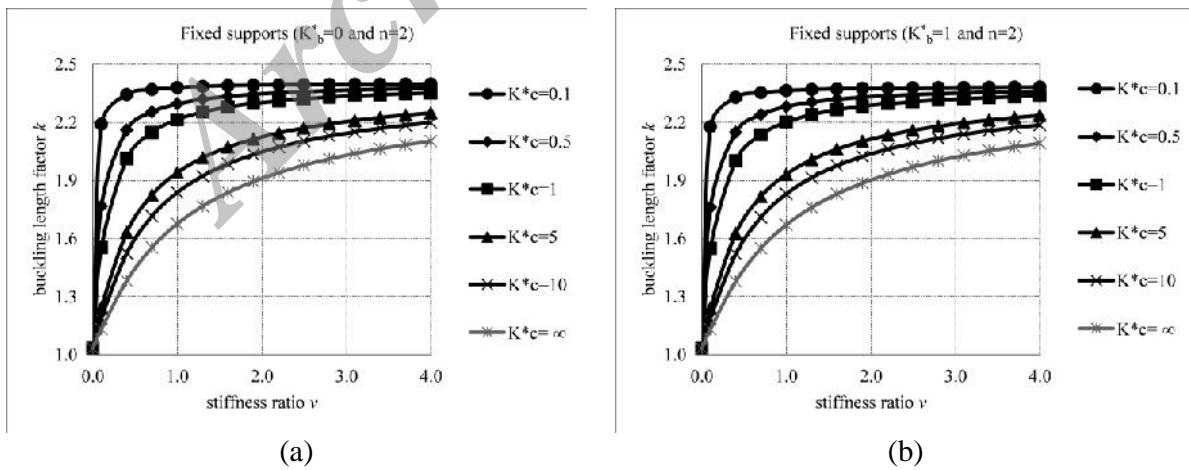


Figure 4. Buckling length factor k versus stiffness ratio v for pinned support frame with non-prismatic columns ($n=2$) and various values of K_c^* and K_b^* ($r=1/2$)



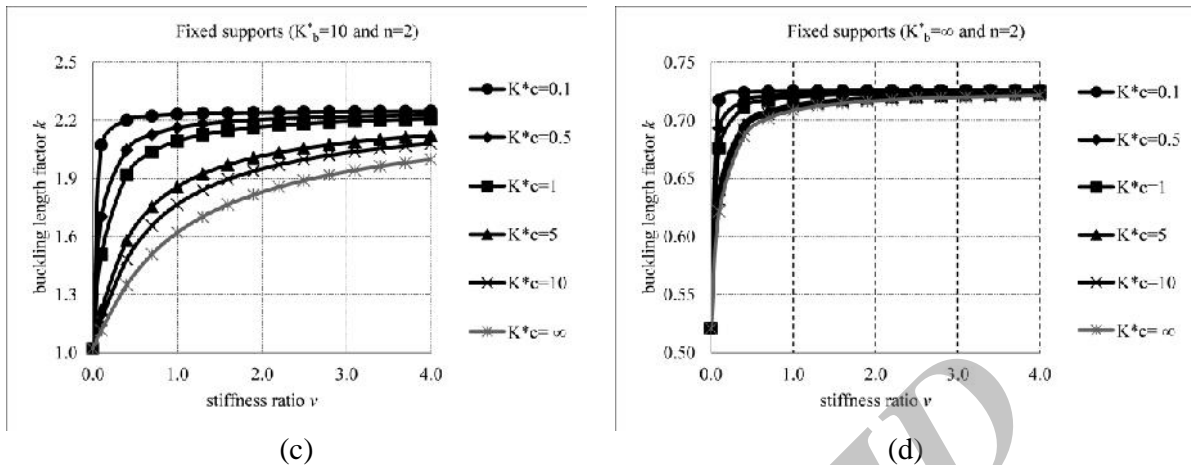


Figure 5. Buckling length factor k versus stiffness ratio v for fixed support frame with non-prismatic columns ($n=2$) and various values of K_c^* and K_b^* ($r=1/2$)

4.3 Solid circular and square section ($n=4$)

The variation of the equivalent buckling length factor k , for the non-uniform frame with pinned supports, with respect to stiffness ratio v for various amounts of the rotational stiffness K_c^* , and various values of the lateral support stiffness K_b^* , and $r=1/2$, are depicted in Fig. 6.

According to Fig. 6(a), in the case of the un-braced frame (i.e. $K_b^*=0$), with pinned supports and $v \rightarrow 0$, the equivalent buckling length factor tends to $k \rightarrow 1.742$, irrespective of the rotational stiffness K_c^* values. This case corresponds to a pinned-fixed sway column (see case (a) in Table (4)). Also, as the stiffness ratio $v \rightarrow \infty$, the equivalent buckling length factor tends to $k \rightarrow \infty$ for all cases of K_c^* .

For intermediate values of the stiffness ratio v and low rotational stiffness amounts (i.e. $K_c^*=0.1, 0.5$ and 1) there is a substantial increase of the equivalent buckling length factor k , which is more pronounced when v tends to low values. This effect is reversed in the case of high rotational stiffness quantities (i.e. $K_c^*=5, 10$ and ∞) as v tends to high values. The same pattern pronounces also in the cases when an lateral support is present (i.e. $K_b^* \neq 0$), as shown in Figs. 6(b) up to 6(d).

In addition, regardless of the rotational stiffness K_c^* quantities, when the stiffness ratio tends to $v \rightarrow 0$, the equivalent buckling length factor tends to $k \rightarrow 1.742, 1.740$ and 0.787 for $K_b^* \rightarrow 1, 10$ and ∞ , respectively. The latter case corresponds to a pinned-fixed non-sway column (see case (e) in Table (4)). Also, for all cases of K_c^* when the stiffness ratio tends to $v \rightarrow \infty$, the equivalent buckling length factor tends to $k \rightarrow 25.847, 8.855$ and 1.125 for $K_b^* \rightarrow 1, 10$ and ∞ , respectively. This last case (i.e. $K_b^* \rightarrow \infty$) corresponds to a pinned-pinned non-sway column (see case (g) in Table (4)).

In Fig. 7, the same plots as above are depicted for the frame with fixed supports. More specifically, in the case of the un-braced frame (i.e. $K_b^*=0$) with fixed supports and $v \rightarrow 0$, the equivalent buckling length factor tends to $k \rightarrow 1.076$, irrespective of the rotational stiffness K_c^* values. This case corresponds to a fixed-fixed sway column (see case (b) in

Table (4)). On the other hand, for $\nu \rightarrow \infty$, the equivalent buckling length factor tends to $k \rightarrow 3.027$, also regardless of the K_c^* amounts. This case corresponds to a fixed-free sway column (see case (d) in Table (4)).

For intermediate values of the stiffness ratio ν and low rotational stiffness amounts (i.e. $K_c^* = 0.1, 0.5$ and 1) there is a significant increase of the equivalent buckling length factor k which is also more pronounced as ν tends to low values. The similar pattern appears also in the cases when an elastic bracing support is present (i.e. $K_b^* \neq 0$), as shown in Figs. 7(b) up to 7(d).

It should be noticed that regardless of the rotational stiffness K_c^* values, whenever the stiffness ratio tends to $\nu \rightarrow 0$, the buckling length factor tends to $k \rightarrow 1.075, 1.070$ and 0.563 for $K_b^* \rightarrow 1, 10$ and ∞ , respectively. The last case (i.e. $K_b^* \rightarrow \infty$) corresponds to a fixed-fixed non-sway column (see case (f) in Table (4)). On the other hand, for $\nu \rightarrow \infty$, the equivalent buckling length factor tends to $k \rightarrow 3.012, 2.882$ and 0.786 for $K_b^* \rightarrow 1, 10$ and ∞ , respectively. The latter case (i.e. $K_b^* \rightarrow \infty$) corresponding to a fixed-pinned non-sway column (see case (h) in Table (4)).

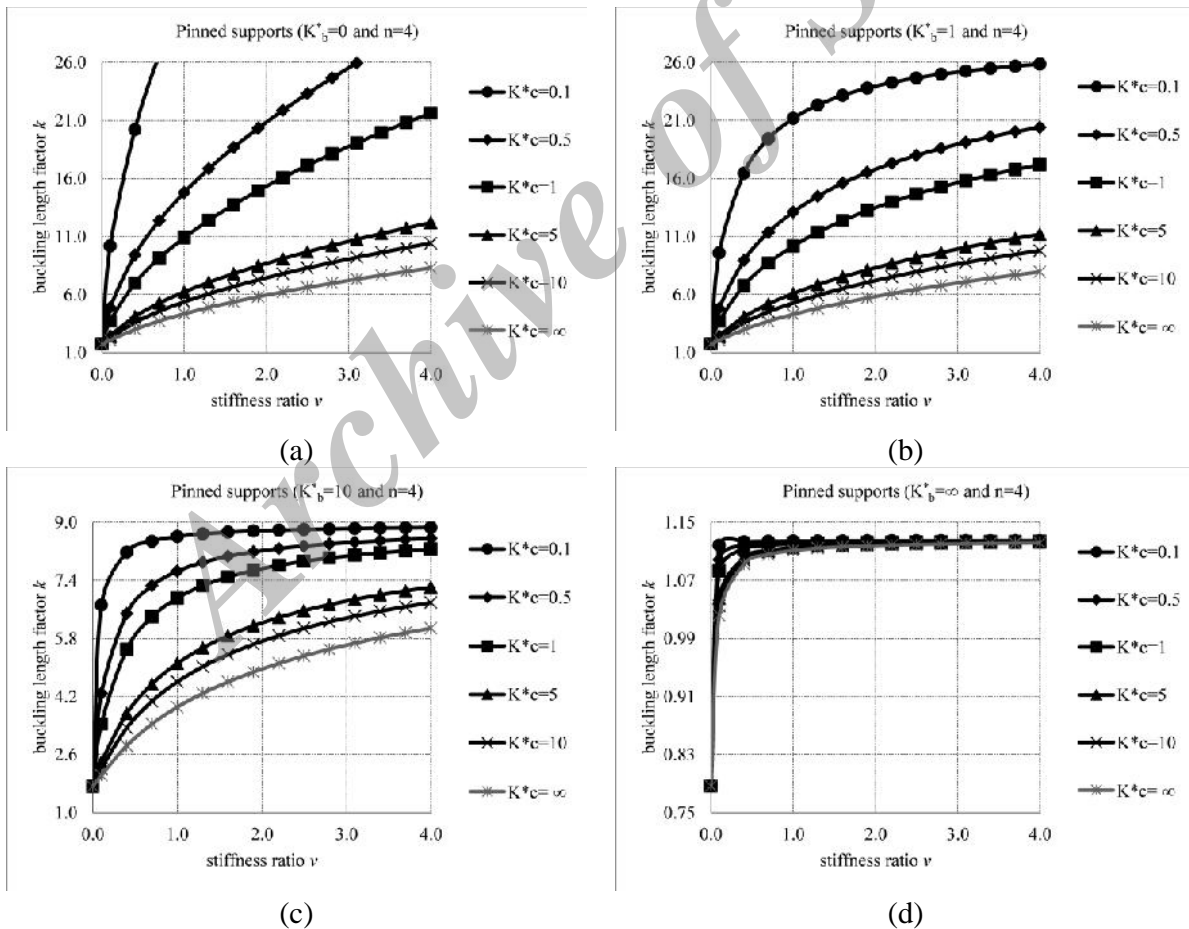


Figure 6. Buckling length factor k versus stiffness ratio ν for pinned support frame with non-prismatic columns ($n=4$) and various values of K_c^* and K_b^* ($r=1/2$)

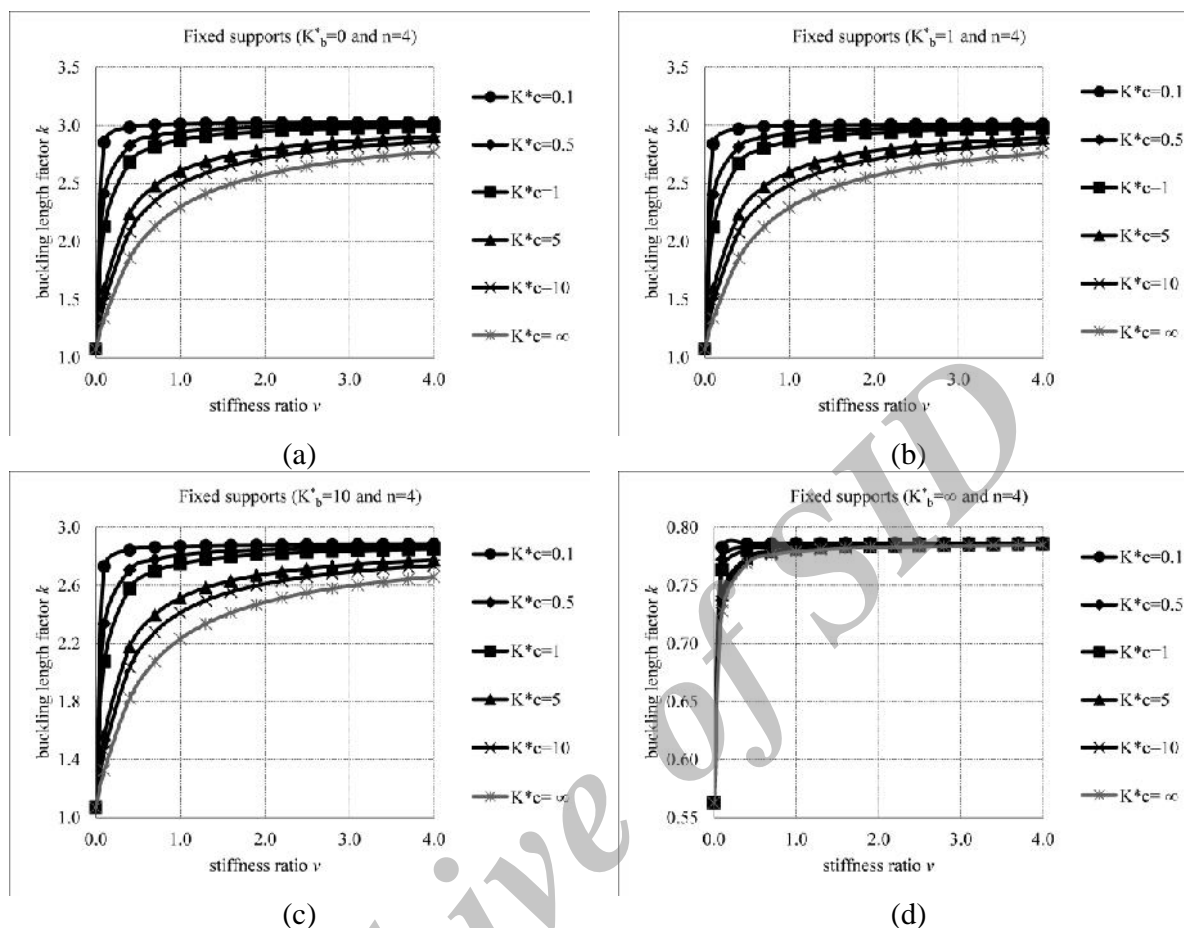


Figure 7. Buckling length factor k versus stiffness ratio v for fixed support frame with non-prismatic columns ($n=4$) and various values of K_c^* and K_b^* ($r=1/2$)

Comparing the Figs. 2 through 7, it is evident that the increase of the lateral stiffness K_b^* from low or zero values (corresponding to the un-braced frames) to infinity (corresponding to the fully-braced frames), will lead to a significant decrease of the equivalent buckling length factor. Consequently, the critical buckling load of the frame increases substantially. The similar pattern follows also in the presence of the rotational stiffness K_c^* . When the rotational stiffness K_c^* reduced from infinity (corresponding to the rigid connections) to very low or zero values (corresponding to the pinned connections), the buckling load of frame changed strongly. These patterns are more apparent when the shape factor increases. Furthermore, these effects are more pronounced in the case of the frame with pinned supports.

From Figs. 2 through 7, it is obvious that the effect of the joint flexibility on the buckling load of the un-braced frame, especially for the shape factor $n=4$, is higher than the braced ones. In addition, a substantial reduction of the frames critical buckling load will be seen, which is caused by effects of the columns shape factor, lateral support, and the flexibility of joints. This reduction is declared for low values of the rotational stiffness as the stiffness ratio v decreases and for high connection flexibility when v increases.

5. NUMERICAL EXAMPLES

To show the robustness of the proposed method, several numerical examples are analyzed in this section. The findings are compared with the other references. Moreover, the effects of taper ratio, shape factor of columns, connection flexibility, and axial stiffness of the lateral support on the critical buckling load of the non-uniform frames are investigated.

5.1 Example 1

The semi-rigid frame with based pinned supports and lateral elastic support K_b , as shown in Fig. 8, was studied recently by Mageirou [25]. The sections of the beam and column are IPE400 and HEB360, respectively. The rotational stiffness of semi-rigid connections is 150kN/rad. The elasticity modulus of materials is also 210GPa. By setting $\nu=3.73454$, $K_c^*=0.06176$ and $K_b^*=0, 11.02548, \infty$ and solving the stability non-dimensional matrix $[K_5]$, i.e. Eq. (A5), the critical buckling loads of the uniform semi-rigid frames are found and presented in Table (5). From Table (5), it is observed the proposed method for computing the critical buckling load has a high accuracy.

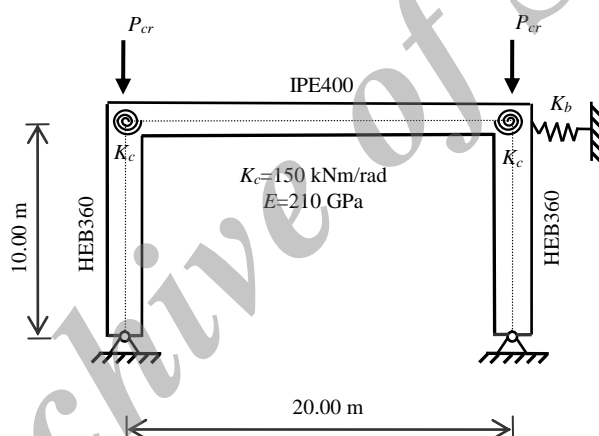


Figure 8. Example 1: uniform frame with pinned supports and semi-rigid connections

Table 5: Critical buckling load P_{cr} (kN)

K_b (kN/m)		Present study	Mageirou [25]	F.E.M.
0	(un-braced)	14.766	14.77	14.77
1000	(semi-braced)	5000.679	5000.01	5000.64
∞	(fully-braced)	8980.670	8980.67	8980.67

5.2 Example 2

At this example, consider the tapered column with various boundary conditions (i.e. Pinned-Pinned, Clamped-Pinned and Clamped-Free) and shape factor $n=2$. The equivalent buckling length factor k of mentioned columns arranged in Table (6). The authors' results show the validity and capability of the proposed method. It is reminded that the solutions of

Ermopoulos are based on the slope-deflection method[26]. From Table (6), it is observed that the equivalent buckling length factor of frame increases, as the taper ratio decreases. In particular, when $r=1$, the presented outcomes for the three cases are identical to the well-known Euler's results.

Table 6: Equivalent critical buckling load factor P_{cr}^* and equivalent buckling length factor k for a tapered column ($n=2$) with different boundary conditions

Taper ratio (r)	l/a	P-P		C-P		C-F	
		$P_{cr}^* = P_{cr} l^2 / EI_m$	k	$P_{cr}^* = P_{cr} l^2 / EI_m$	k	$P_{cr}^* = P_{cr} l^2 / EI_m$	k
1	0.0	9.867	1.000	20.191	0.699	2.467	2.00
		-	-	-	-	-	-
2/3	0.5	9.645	1.012	19.637	0.709	2.030	2.205
		(9.62)	(1.012)	(19.64)	(0.709)	(2.01)	(2.211)
1/2	1.0	9.241	1.033	18.715	0.726	1.705	2.406
		(9.22)	(1.034)	(18.70)	(0.726)	(1.69)	(2.415)
1/3	2.0	8.427	1.082	16.816	0.766	1.274	2.783
		-	-	-	-	-	-
1/4	3.0	7.755	1.128	15.257	0.804	1.009	3.128
		-	-	-	-	-	-
1/6	5.0	6.784	1.206	13.022	0.872	0.705	3.741
		(6.77)	(1.207)	(13.02)	(0.871)	(0.68)	(3.784)

Results in parenthesis are taken from Ermopoulos [26]

5.3 Example 3

Consider the semi-rigid portal frame shown in Fig. 9. The beam has a uniform built-up section consisting of four angles 45×5 connected by lacing bars. The non-prismatic columns consist of two symmetric tees, IPE270, connect by lacing bar. The elasticity modulus of the materials is 210GPa. The mentioned frame with rigid connection (i.e. $K_c^* = \infty$) was investigated by Kounadis and Ermopoulos [6]. By bifurcation analysis, the dimensionless critical buckling load factor of the frame is founded as 1.141. In this paper, solving the stability determinant $[K_3]$ (i.e. Eq. (A3)) by setting $r=5.25/15.75=1/3$, $v=(20655 \times 10)/(34900 \times 15.75)=0.37577$, $K_c^* = \infty$ and $K_b^* = 0$ will be computed $\rho_{cr}=1.1409$ and $P_{cr}^* = 1.5518$, which is very close to the value obtained by Kounadis and Ermopoulos [6]. For the corresponding frame, having uniform columns with a constant moment of inertia I_m and utilizing of the unknown dimensionless constant matrix $[K_5]$ (i.e. Eq. (A5)), the dimensionless equivalent critical load is calculated as $P_{cr}^* = 1.3451$. Accordingly, the critical buckling load of the non-uniform frame is 15% higher than the corresponding uniform frame. In order to demonstrate the effect of the joint flexibility, the mentioned frame with $K_c^* = 3$ is analyzed. In this case, the equivalent critical buckling load factor is

obtained as $P_{cr}^* = 0.7266$. As a result, the flexibility of connection reduces the load-carrying capacity approximately 53% and 46% with respect to the similar rigid non-uniform and uniform frame, respectively.

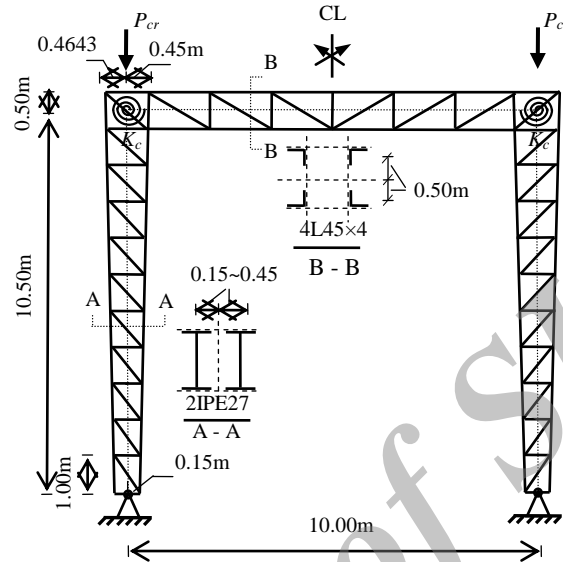


Figure 9. Example 3: Geometry and cross-sectional properties of un-braced semi-rigid portal frame with tapered columns

In the next study, the corresponding non-uniform semi-rigid frame with fixed supports is investigated. By utilizing of the matrix $[K_4]$ (i.e. Eq. (A4)), the equivalent critical buckling load factor of this frame is evaluated as $P_{cr}^* = 2.4573$. It is worth emphasizing that the rigidity of the bases, increase the load-carrying capacity more than 238% (i.e. ≈ 3.4 times more) with respect to the corresponding frame with pinned supports.

5.4 Example 4

In order to demonstrate the effect of the elastic bracing system, the braced non-uniform steel frames, as shown in Fig. 10, are studied. The structural modulus of elasticity is 210GPa. In addition, the rotational stiffness of semi-rigid beam-to-column connections, K_c , in both frames is assumed to be constant and equal to 2198700 kN.cm/rad. Accordingly, the dimensionless rotational stiffness K_c^* is obtained as below:

$$K_c^* = \frac{K_c l_b}{EI_b} = \frac{2198700 \times 1000}{21000 \times 34900} = 3$$

Both bracing members consist of two L30x5 angle sections (with area $A_d = 2 \times 2.78 \text{ cm}^2$). As a result, the lateral stiffness, K_b , and the dimensionless lateral stiffness, K_b^* , are evaluated, in the below form:

$$K_b = \frac{EA_d l_b^2}{l_d^3} = \frac{21000 \times 2 \times 2.78 \times 1000^2}{1450^3} = 38.30 \text{ kN/cm}$$

$$K_b^* = \frac{K_b h^3}{EI_c} \times r^2 = \frac{38.30 \times 1575^3}{21000 \times 20655} \times \left(\frac{1}{3}\right)^2 = 38.31$$

Solving the stability determinant $[K_3]$ (i.e. Eq. (A3)), with $r=1/3$, $v=0.37577$, $K_c^*=3$ and $K_b^*=38.31$, $\rho_{cr}=2.9612$ will be computed. Consequently, using Eqs. (11) and (12), will lead to $P_{cr}=14193$ kN and $k=1.046$, respectively. The critical buckling load of the similar unbraced non-uniform with semi-rigid connection is obtained as 1143kN. It is worth emphasizing that the bracing members increase the critical buckling load more than 1141% (i.e. ≈ 12.5 times more). Furthermore, for the corresponding braced frame, having uniform columns with a constant moment of inertia I_m ($r=1$) and semi-rigid connections, the critical load is equal to 17080 kN, which is unpredictably greater than the same non-uniform frame by about 20%.

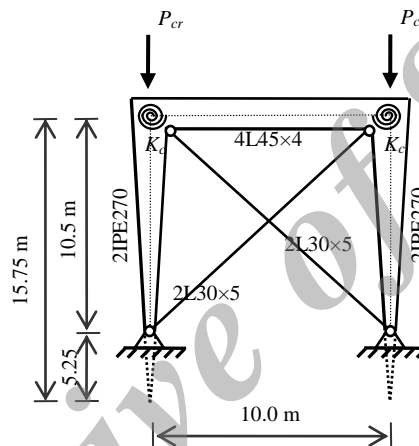


Figure 10. Example 4: Geometry and cross-sectional properties of braced non-uniform steel frames

5.5 Example 5

Finally, consider the semi-rigid portal frame as shown Fig. 11. The beam has a uniform square section, and the columns have a taper square section. In this case, the columns' moment of inertia varies according to the law given in Eq. (1), with $n=4$, whereas the beam has a constant moment of inertia. The elasticity modulus of the materials is 210GPa. Solving the stability determinant, $[K_1]$ (i.e. Eq. (A1)), and employing $r=4/12=1/3$, $v=(10^4/12 \times 12)/(30^4/12 \times 12)=1/81$, $K_c^*=3$ and $K_b^*=0$ will lead to $\rho_{cr}=4.3291$. The non-dimensional equivalent critical buckling load is obtained as $P_{cr}^* = 4.6852$. For the corresponding frame having uniform columns with a constant moment of inertia I_m , by utilizing the matrix $[K_5]$ (i.e. Eq. (A5)), and setting $v=(20^4/12 \times 12)/(30^4/12 \times 8)=8/27$, $K_c^*=3$ and $K_b^*=0$, the dimensionless equivalent critical buckling load is calculated as $P_{cr}^*=7.5855$. Accordingly, the load-carrying capacity of the semi-rigid frame with taper square columns is smaller than that of the corresponding semi-rigid frame with uniform square columns by about 38%.

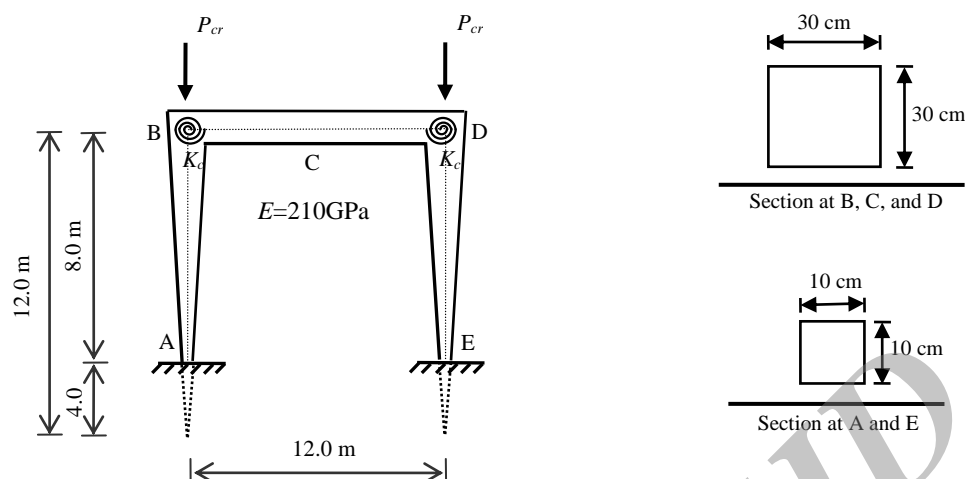


Figure 11. Example 5: Geometry and cross-sectional properties of un-braced semi-rigid portal frame with square tapered columns

6. CONCLUSIONS

This paper was devoted to the stability analysis of a general portal frame. For the first time, a closed-form solution for stability analysis of a semi-rigid frame with non-uniform column and elastic bracing was obtained. The proposed formulation can compute the "exact" critical load, and corresponding equivalent buckling length of non-uniform frames with semi-rigid connections and elastic bracing system. Moreover, the presented expressions can be used for the non-prismatic column with various end boundary conditions. Parametric studies for simple non-uniform frames reveal the effect of tapered members, flexibility of joint, and elastic bracing on their buckling load. Comparing the outcomes with the previous published results shows the accuracy, validity and capabilities of the proposed approach. According to all the findings in this study, including parametric and numerical solution, the following points are concluded:

1. The combined effect of the shape factor, taper ratio, elastic bracing system, and joint flexibility on the critical buckling load and corresponding equivalent buckling length factor of portal steel frames is very significant. As a result, these effects should be considered in design of such structures.

2. The connection flexibility will reduce critical buckling load of the frame. Consequently, it increases the corresponding equivalent buckling length factor. These effects are similar to the elastic bracing system.

3. As the taper ratio decreases, the equivalent critical buckling load factor decreases, while the corresponding equivalent buckling length factor as well as critical buckling load increases.

4. The equivalent buckling length factor of the non-uniform portal frames will increase, when the shape factor as well as stiffness ratio increases. For the un-braced frames with pinned supports, this effect is even more pronounced.

5. In some cases, the critical buckling load of non-uniform frames is lesser than the corresponding frame with uniform columns.

7. APPENDIX A

The unknown constants matrixes, \mathbf{K}_1 and \mathbf{K}_2 , for the fixed and pinned supports' frame with shape factor $n = 4$, respectively, are defined below:

$$K_1 = \begin{bmatrix} r \sin \rho & r \cos \rho & r & 1 & 0 & 0 & 0 & 0 & 0 & 0 & 0 \\ \sin \rho - \rho \cos \rho & \cos \rho + \rho \sin \rho & 1 & 0 & 0 & 0 & 0 & 0 & 0 & 0 & 0 \\ 0 & 0 & 0 & 0 & 0 & 0 & r \sin \rho & r \cos \rho & r & 1 & 0 \\ 0 & 0 & 0 & 0 & 0 & 0 & \sin \rho - \rho \cos \rho & \cos \rho + \rho \sin \rho & 1 & 0 & 0 \\ 0 & 0 & 0 & 0 & v^2 & v & 1 & 0 & 0 & 0 & 0 \\ \sin(r\rho) & \cos(r\rho) & 1 & 1 & 0 & 0 & 0 & -\sin(r\rho) & -\cos(r\rho) & -1 & -1 \\ 0 & 0 & -\rho^2 & 0 & 0 & 0 & 0 & K_b^* \sin(r\rho) & K_b^* \cos(r\rho) & K_b^* - \rho^2 & K_b^* \\ \rho^2 \sin(r\rho) & \rho^2 \cos(r\rho) & 0 & 0 & 0 & 2r^2 & 0 & 0 & 0 & 0 & 0 \\ K_c^* (\sin(r\rho) - r\rho \cos(r\rho)) & K_c^* (\cos(r\rho) + r\rho \sin(r\rho)) & K_c^* & 0 & 0 & 2v & -K_c^* & 0 & 0 & 0 & 0 \\ 0 & 0 & 0 & 0 & -6vr^2 & -2r^2 & 0 & \rho^2 \sin(r\rho) & \rho^2 \cos(r\rho) & 0 & 0 \\ 0 & 0 & 0 & 0 & 3v^2(K_c^* + 2) & 2v(K_c^* + 1) & K_c^* & K_c^* (r\rho \cos \rho - \sin(r\rho)) & -K_c^* (\cos(r\rho) + r\rho \sin(r\rho)) & -K_c^* & 0 \end{bmatrix} \quad (A1)$$

$$K_2 = \begin{bmatrix} r \sin \rho & r \cos \rho & r & 1 & 0 & 0 & 0 & 0 & 0 & 0 & 0 \\ \sin \rho & \cos \rho & 0 & 0 & 0 & 0 & 0 & 0 & 0 & 0 & 0 \\ 0 & 0 & 0 & 0 & 0 & 0 & r \sin \rho & r \cos \rho & r & 1 & 0 \\ 0 & 0 & 0 & 0 & 0 & 0 & -\sin \rho & -\cos \rho & 0 & 0 & 0 \\ 0 & 0 & 0 & 0 & v^2 & v & 1 & 0 & 0 & 0 & 0 \\ \sin(r\rho) & \cos(r\rho) & 1 & 1 & 0 & 0 & 0 & -\sin(r\rho) & -\cos(r\rho) & -1 & -1 \\ 0 & 0 & -\rho^2 & 0 & 0 & 0 & 0 & K_b^* \sin(r\rho) & K_b^* \cos(r\rho) & K_b^* - \rho^2 & K_b^* \\ \rho^2 \sin(r\rho) & \rho^2 \cos(r\rho) & 0 & 0 & 0 & 2r^2 & 0 & 0 & 0 & 0 & 0 \\ K_c^* (\sin(r\rho) - r\rho \cos(r\rho)) & K_c^* (\cos(r\rho) + r\rho \sin(r\rho)) & K_c^* & 0 & 0 & 2v & -K_c^* & 0 & 0 & 0 & 0 \\ 0 & 0 & 0 & 0 & -6vr^2 & -2r^2 & 0 & \rho^2 \sin(r\rho) & \rho^2 \cos(r\rho) & 0 & 0 \\ 0 & 0 & 0 & 0 & 3v^2(K_c^* + 2) & 2v(K_c^* + 1) & K_c^* & K_c^* (r\rho \cos \rho - \sin(r\rho)) & -K_c^* (\cos(r\rho) + r\rho \sin(r\rho)) & -K_c^* & 0 \end{bmatrix} \quad (A2)$$

$$\text{in which, } \rho^2 = \frac{Pa^2}{EI_c}, \quad v = \frac{I_c l_b}{I_b h}, \quad r = \frac{a}{h}, \quad K_b^* = \frac{K_b h^3}{EI_c} r^2, \quad K_c^* = \frac{K_c l_b}{EI_b}.$$

The unknown constants matrixes, \mathbf{K}_3 and \mathbf{K}_4 , for the fixed and pinned supports' frame with shape factor $n = 2$, respectively, have the next values:

$$K_3 = \begin{bmatrix} 0 & 1 & r & 1 & 0 & 0 & 0 & 0 & 0 & 0 & 0 \\ \rho & 1/2 & r & 0 & 0 & 0 & 0 & 0 & 0 & 0 & 0 \\ 0 & 0 & 0 & 0 & 0 & 0 & 0 & 0 & 1 & r & 1 \\ 0 & 0 & 0 & 0 & 0 & 0 & \rho & 1/2 & r & 0 & 0 \\ 0 & 0 & 0 & 0 & v^2 & v & 1 & 0 & 0 & 0 & 0 \\ S & C & 1 & 1 & 0 & 0 & 0 & -S & -C & -1 & -1 \\ 0 & 0 & -(\rho^2 + 1/4) & 0 & 0 & 0 & 0 & K_b^* S & K_b^* C & K_b^* - (\rho^2 + 1/4) & K_b^* \\ (\rho^2 + 1/4)S & (\rho^2 + 1/4)C & 0 & 0 & 0 & 2r^2 & 0 & 0 & 0 & 0 & 0 \\ K_c^* (S/2 + \rho C) & K_c^* (C/2 - \rho S) & K_c^* & 0 & 0 & 2v & -K_c^* & 0 & 0 & 0 & 0 \\ 0 & 0 & 0 & 0 & -6vr^2 & -2r^2 & 0 & (\rho^2 + 1/4)S & (\rho^2 + 1/4)C & 0 & 0 \\ 0 & 0 & 0 & 0 & 3v^2(K_c^* + 2) & 2v(K_c^* + 1) & K_c^* & -K_c^* (S/2 + \rho C) & -K_c^* (C/2 - \rho S) & -K_c^* & 0 \end{bmatrix} \quad (A3)$$

$$K_4 = \begin{bmatrix} 0 & 1 & r & 1 & 0 & 0 & 0 & 0 & 0 & 0 & 0 \\ 0 & -(\rho^2+1/4) & 0 & 0 & 0 & 0 & 0 & 0 & 0 & 0 & 0 \\ 0 & 0 & 0 & 0 & 0 & 0 & 0 & 0 & 1 & r & 1 \\ 0 & 0 & 0 & 0 & 0 & 0 & 0 & 0 & -(\rho^2+1/4) & 0 & 0 \\ 0 & 0 & 0 & 0 & v^2 & v & 1 & 0 & 0 & 0 & 0 \\ S & C & 1 & 1 & 0 & 0 & 0 & -S & -C & -1 & -1 \\ 0 & 0 & -(\rho^2+1/4) & 0 & 0 & 0 & 0 & K_b^*S & K_b^*C & K_b^* - (\rho^2+1/4) & K_b^* \\ (\rho^2+1/4)S & (\rho^2+1/4)C & 0 & 0 & 0 & 2r^2 & 0 & 0 & 0 & 0 & 0 \\ K_c^*(S/2+\rho C) & K_c^*(C/2-\rho S) & K_c^* & 0 & 0 & 2v & -K_c^* & 0 & 0 & 0 & 0 \\ 0 & 0 & 0 & 0 & -6v^2 & -2r^2 & 0 & (\rho^2+1/4)S & (\rho^2+1/4)C & 0 & 0 \\ 0 & 0 & 0 & 0 & 3v^2(K_c^*+2) & 2v(K_c^*+1) & K_c^* & -K_c^*(S/2+\rho C) & -K_c^*(C/2-\rho S) & -K_c^* & 0 \end{bmatrix} \quad (A4)$$

The following parameters are used in the last matrices:

$$\rho^2 = \frac{Pa^2}{EI_c} - \frac{1}{4}, \quad v = \frac{I_c l_b}{I_b h}, \quad r = \frac{a}{h}, \quad K_b^* = \frac{K_b h^3}{EI_c} r^2, \quad K_c^* = \frac{K_c l_b}{EI_b}, \quad S = \sqrt{\frac{1}{r}} \sin\left(\rho \ln\left(\frac{1}{r}\right)\right), \\ C = \sqrt{\frac{1}{r}} \cos\left(\rho \ln\left(\frac{1}{r}\right)\right).$$

The unknown constants matrixes, \mathbf{K}_5 and \mathbf{K}_6 , for the fixed and pinned supports' frame with shape factor $n = 0$, respectively are defined by the next relationships:

$$K_5 = \begin{bmatrix} 0 & 1 & 0 & 1 & 0 & 0 & 0 & 0 & 0 & 0 & 0 \\ \rho & 0 & 1 & 0 & 0 & 0 & 0 & 0 & 0 & 0 & 0 \\ 0 & 0 & 0 & 0 & 0 & 0 & 0 & 0 & 1 & 0 & 1 \\ 0 & 0 & 0 & 0 & 0 & 0 & 0 & \rho & 0 & 1 & 0 \\ 0 & 0 & 0 & 0 & v^2 & v & 1 & 0 & 0 & 0 & 0 \\ \sin \rho & \cos \rho & 1 & 1 & 0 & 0 & 0 & -\sin \rho & -\cos \rho & -1 & -1 \\ 0 & 0 & -\rho^2 & 0 & 0 & 0 & 0 & K_b^* \sin \rho & K_b^* \cos \rho & K_b^* - \rho^2 & K_b^* \\ \rho^2 \sin \rho & \rho^2 \cos \rho & 0 & 0 & 0 & 2 & 0 & 0 & 0 & 0 & 0 \\ K_c^* \rho \cos \rho & -K_c^* \rho \sin \rho & K_c^* & 0 & 0 & 2v & -K_c^* & 0 & 0 & 0 & 0 \\ 0 & 0 & 0 & 0 & -6v & -2 & 0 & \rho^2 \sin \rho & \rho^2 \cos \rho & 0 & 0 \\ 0 & 0 & 0 & 0 & 3v^2(K_c^*+2) & 2v(K_c^*+1) & K_c^* & -K_c^* \rho \cos \rho & K_c^* \rho \sin \rho & -K_c^* & 0 \end{bmatrix} \quad (A5)$$

$$K_6 = \begin{bmatrix} 0 & 1 & 0 & 1 & 0 & 0 & 0 & 0 & 0 & 0 & 0 \\ 0 & -1 & 0 & 0 & 0 & 0 & 0 & 0 & 0 & 0 & 0 \\ 0 & 0 & 0 & 0 & 0 & 0 & 0 & 0 & 1 & 0 & 1 \\ 0 & 0 & 0 & 0 & 0 & 0 & 0 & 0 & -1 & 0 & 0 \\ 0 & 0 & 0 & 0 & v^2 & v & 1 & 0 & 0 & 0 & 0 \\ \sin \rho & \cos \rho & 1 & 1 & 0 & 0 & 0 & -\sin \rho & -\cos \rho & -1 & -1 \\ 0 & 0 & -\rho^2 & 0 & 0 & 0 & 0 & K_b^* \sin \rho & K_b^* \cos \rho & K_b^* - \rho^2 & K_b^* \\ \rho^2 \sin \rho & \rho^2 \cos \rho & 0 & 0 & 0 & 2 & 0 & 0 & 0 & 0 & 0 \\ K_c^* \rho \cos \rho & -K_c^* \rho \sin \rho & K_c^* & 0 & 0 & 2v & -K_c^* & 0 & 0 & 0 & 0 \\ 0 & 0 & 0 & 0 & -6v & -2 & 0 & \rho^2 \sin \rho & \rho^2 \cos \rho & 0 & 0 \\ 0 & 0 & 0 & 0 & 3v^2(K_c^*+2) & 2v(K_c^*+1) & K_c^* & -K_c^* \rho \cos \rho & K_c^* \rho \sin \rho & -K_c^* & 0 \end{bmatrix} \quad (A6)$$

$$\text{in which, } \rho^2 = \frac{Pl_c^2}{EI_c}, \quad \nu = \frac{I_c l_b}{I_b l_c}, \quad K_b^* = \frac{K_b l_c^3}{EI_c}, \quad K_c^* = \frac{K_c l_b}{EI_b}.$$

REFERENCES

1. Bažant ZP, Cedolin L. *Stability of Structures: Elastic, Inelastic, Fracture and Damage Theories*. World Scientific, 2010.
2. Timoshenko SP, Gere JM. *Theory of Elastic Stability*. Dover Publications, 2009.
3. Chen WF, Lui EM. *Stability Design of Steel Frames*, CRC Press, 1991.
4. Euler L. Die altitudine colomnarum sub proprio pondere corruentium, 1778.
5. Gere JM, Carter WO. Critical buckling loads for tapered columns, *Journal of the Structural Division*, **88**(1962) 1-12.
6. Ermopoulos JC, Kounadis AN. Stability of frames with tapered built-up members, *Journal of Structural Engineering*, **111**(1985) 1979-92.
7. Raftoyiannis IG, Ermopoulos JC. Stability of tapered and stepped steel columns with initial imperfections, *Engineering Structures*, **27**(2005) 1248-57.
8. Ermopoulos JC. Buckling length of framed compression members with semirigid connections, *Journal of Constructional Steel Research*, **18**(1991) 139-54.
9. Al-Sadder SZ. Exact expressions for stability functions of a general non-prismatic beam-column member, *Journal of Constructional Steel Research*, **60**(2004) 1561-84.
10. Al-Sadder SZ, Qasravi HY. Exact secant stiffness matrix for non-prismatic beam-columns with elastic semi-rigid joint connections, *Emirates Journal for Engineering Research*, **9**(2004) 127-35.
11. Li QS. Exact solutions for buckling of non-uniform columns under axial concentrated and distributed loading, *European Journal of Mechanics - A/Solids*, **20**(2001) 485-500.
12. Li QS. Analytical solutions for buckling of multi-step non-uniform columns with arbitrary distribution of flexural stiffness or axial distributed loading, *International Journal of Mechanical Sciences*, **43**(2001) 349-66.
13. Coşkun SB, Atay MT. Determination of critical buckling load for elastic columns of constant and variable cross-sections using variational iteration method, *Computers & Mathematics with Applications*, **58**(2009) 2260-6.
14. Darbandi SM, Firouz-Abadi RD, Haddadpour H. Buckling of variable section columns under axial loading, *Journal of Engineering Mechanics*, **136** (2010) 472-6.
15. O'Rourke M, Zebrowski T. Buckling load for nonuniform columns, *Computers & Structures*, **7**(1977) 717-20.
16. Iremonger MJ. Finite difference buckling analysis of non-uniform columns, *Computers & Structures*, **12**(1980) 741-8.
17. Bazeos N, Karabalis DL. Efficient computation of buckling loads for plane steel frames with tapered members, *Engineering Structures*, **28**(2006) 771-5.
18. Li GQ, Li JJ. Buckling analysis of tapered lattice columns using a generalized finite element, *Communications in Numerical Methods in Engineering*, **20**(2004) 479-88.

19. Marques L, Taras A, Simões da Silva L, Greiner R, Rebelo C. Development of a consistent buckling design procedure for tapered columns, *Journal of Constructional Steel Research* **72**(2012) 61-74.
20. Smith WG. Analytic solutions for tapered column buckling, *Computers & Structures*, **28**(1988) 677-81.
21. Arbabi F, Li F. Buckling of variable cross-section columns: integral-equation approach. *Journal of Structural Engineering*, **117**(1991) 2426-41.
22. Rezaiee-Pajand M, Moayedian M. Nonprismatic beam and column design tables for nonlinear analysis, *Asian Journal of Structural Engineering*, **1**(1995) 337-49.
23. Rezaiee-Pajand M, Moayedian M. Explicit stiffness of tapered and monosymmetric I beam-columns, *International Journal of Engineering*, **13**(2000) 1-18.
24. Huang Y, Li X-F. An analytic approach for exactly determining critical loads of buckling of non-uniform columns, *International Journal of Structural Stability and Dynamics*, **12**(2012) 1250027.
25. Mageirou GE. Contribution to design of multi-story steel frames against flexural buckling, PhD Thesis, National Technical University of Athens, 2011.
26. Ermopoulos JC. Equivalent buckling length of non-uniform members, *Journal of Constructional Steel Research*, **42**(1997) 141-58.

Archive of SID